

Prestack time migration applied to marine P-SV seismic waves

A. Sollid, B. O. Ekren* and B. Arntsen; Statoil Research Centre, Norway

Summary

P-SV mode converted seismic waves require special processing due to asymmetrical raypaths. Since standard CMP processing is not applicable to P-SV data, sorting into Common Conversion Point (CCP) gathers is necessary before stacking and migration. We omit the explicit CCP sorting using a common-offset Kirchhoff time migration adapted to handle P-SV converted waves.

Reflectors on a stacked P-SV section often deviate from P-P events in character and amplitude, sometimes making correlation between the two sections difficult. To reduce this problem, the migration scheme can be designed to output P-SV migrated constant-offset sections in P-P travel time. The data is smoothly compressed in a time variant manner according to the depth- and laterally variant α/β ratios. The P-wave RMS velocities utilized in the migration may be obtained from stacking velocity analysis of conventional P-wave data or the vertical particle velocity component acquired at the sea bottom. The S-wave RMS velocities may be estimated via the α/β ratios and Dix' equation. More accurate S-velocities are achieved by migrating the data to S-S travel time, backing out the S-S velocity function in the migrated data and picking new migration velocities on S-S time scaled gathers.

The horizontal in-line particle velocity component of a sea bottom acquired seismic data set from the Tommeliten Alpha field offshore Norway contains strong shear-wave events, interpreted as P-SV waves (Granli et al. 1995). The aim of this survey was to improve the seismic image of the reservoir, located beneath gas filled overburden sediments. Gas in the overburden slows down, attenuates and severely scatters the conventional P-waves. Therefore, P-waves do not map the reservoir zone. In this paper we show that prestack time migration adapted to P-SV waves significantly reduce the zone of uncertainty and thereby improves the imaging of the reservoir at Tommeliten Alpha. We compare the results from prestack migration and a P-SV DMO method (Harrison 1992).

Introduction

CMP sorted P-SV converted seismic data suffer from severe reflection point smearing, even for horizontal reflectors. The conversion point is offset from the midpoint towards the receiver, see Figure 1. For a given source-to-receiver offset the lateral position of the conversion point varies with depth. Consequently, conventional midpoint processing is inadequate. Several papers have addressed processing techniques for P-SV seismic data aiming at construction of stacked zero-offset sections. A P-SV stack can in practice be migrated using conventional poststack migration schemes (Harrison 1992).

Instead of CMP-sorting, the P-SV prestack data should

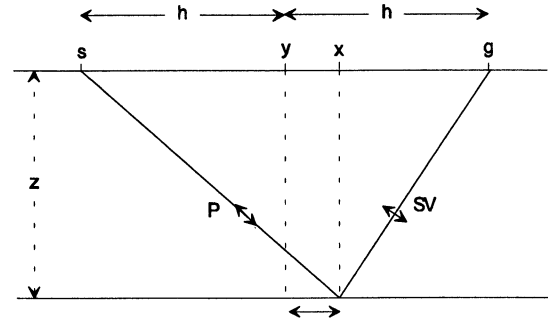


Figure 1: Ray geometry for P-SV converted waves.

be sorted into Common Conversion Point (CCP) gathers. A pragmatic scheme to estimate the conversion point was suggested by From et al. (1985). They used an approximation for the lateral position x of the conversion point

$$x \approx y + \left(\frac{\alpha/\beta - 1}{\alpha/\beta + 1} \right) h, \quad (1)$$

where h is the half-offset and y is the midpoint between source and receiver. This equation corresponds to a trace-by-trace sorting. The approximation error is especially large for shallow reflectors.

A more accurate approach was described by Tessmer and Behle (1988). They derived a fourth order polynomial equation describing the conversion point in a single homogeneous flat layer given the depth and the α/β ratio. In the multi layered case they used RMS velocities, corresponding to a straight-ray approximation. The method does a sample-by-sample sorting into CCP gathers.

Dip moveout (DMO) attempts to remove reflection point smearing due to dipping layers. Harrison (1992) derived an integral-summation based DMO algorithm which properly correct for the reflection point dispersal in P-SV data.

Common offset P-SV Kirchhoff time migration

Kirchhoff time migration may be expressed in midpoint coordinate ($y = (g+s)/2$) and half-offset ($h = (g-s)/2$) domain as

$$I(\tau, y, h) = \int W(\tau, y, b, h) D(t_a + t_g I \tau, y, b, h) db,$$

where I is the image; W is a weighting function; $D^{(2)}$ is the time derivative of the input data; T is the travelttime

Prestack time migration of P-SV data

depth; t_s is the traveltime from source position s to the image point; t_g is the traveltime from image point to receiver position g . The lateral offset from the midpoint to the imagepoint is denoted $b = x - z$, where the image point is located at (x, z) in the earth. Similar to conventional Kirchhoff time migration for seismic P-waves, P-SV waves may be migrated by performing a weighted summation of amplitudes along diffraction curves as described in equation (2). In our-scheme, where the aim is to make structural pictures of the earth's subsurface, we assume that the medium is sufficiently one-dimensional so that a time migration scheme using RMS velocities is applicable. This implies that the travel times are computed analytically using a straight ray approximation.

Filter operation: In 2D migration a temporal half-derivative filter is applied to the input data. This is done in the frequency domain, $D(w, y, h) = \sqrt{-i\omega} P(w, y, h)$, where P is the P-SV wave field.

Travel time computations: In marine multicomponent acquisition the source is a conventional airgun array towed by a vessel at the sea surface, while the geophones are situated at the seabed. If the seabed is relatively flat, the water column is easily counted for in the prestack migration. The parameter t_{PS} denotes the P-SV traveltime from the source s at the sea surface to the image point located at (x, z) in the earth, back to the receiver g is situated at the sea floor. The expression for the traveltime applicable for common offset P-SV time migration reads

$$t_{PS} = \sqrt{\left(\frac{\tau_{PP} + \tau_w}{2}\right)^2 + \left(\frac{h+b}{\alpha_{RMS}}\right)^2} + \sqrt{\left(\frac{\tau_{SS}}{2}\right)^2 + \left(\frac{h-b}{\beta_{RMS}}\right)^2}. \quad (3)$$

where α_{RMS} and β_{RMS} are the RMS velocities for P-waves and S-waves respectively; τ_{PP} and τ_{SS} denote the vertical travel time from the seabed to the reflection point and back to the seabed for P-waves and S-waves. The two-way vertical traveltime in the water layer is τ_w . In practice, to mimic a time migration scheme, one of the traveltime depth parameters, let us say τ_{PP} , is sampled with a constant sampling interval Δr_{pp} . The parameter τ_{SS} is then related to τ_{PP} through $\gamma = \alpha/\beta$,

$$\tau_{SS}(y, n) = \sum_{i=1}^{n-1} \Delta \tau_{PP} | \gamma(y, i).$$

The index n is the sample number. The P-SV travel time depth is given by $\tau_{PS} = \frac{1}{2}(\tau_{PP} + \tau_{SS})$. We can now display the migrated data in P-P traveltimes, $I(\tau_{PP}, y, h)$, which may be directly compared to the P-wave migrated stack. Alternatively, we may sample τ_{SS} or τ_{PS} uniformly and output the image in S-S or P-S traveltimes; $I(\tau_{SS}, y, h)$ or $I(\tau_{PS}, y, h)$. This simple time scaling mechanism will smoothly compress (to P-P time) or stretch (to S-S time) the output image according to the velocity ratio γ .

Weights: The only weight applied to the data prior to summation is $W = \frac{1}{2}(\cos \theta_s + \cos \theta_g)$, where θ_s is the angle between incident straight ray and the vertical axis

while θ_g is the angle between the reflected straight ray and the vertical axis.

Aliasing: To avoid operator aliasing, the dip response is limited according to the maximum frequency of the data (Harrison, 1992). Impulse responses are shown in Figure 2 where the dip is restricted to 60°. The input data was a trace containing 5 zero phase wavelets at 0.5, 1.0, 1.5, 2.0 and 2.5 seconds (the crosses in Figure 2 indicate the positions of the wavelets). Note that the impulse responses are asymmetrical and offset from the midpoint.

Velocity analysis: Prestack P-SV time migration is more sensitive to velocity errors than P-P prestack time migration. Accurate estimates of the α/β ratios are crucial to get an accurate estimate of the image points. Often, no shear wave velocity information is available in the area. The α/β ratios may be estimated by event correlation between the migrated P-stack and the P-SV stack generated via conventional CCP sorting. Alternatively, the choice of α/β ratios may be estimated by iterative prestack migration of near offset sections. The near offset migration results are not sensitive to α and β , but indeed to the α/β ratio. After each migration the horizons in the migrated near offset sections scaled to P-P time) are correlated to horizons in the P-wave migrated stack section. The α/β ratios are updated according to the correlation mismatch at each horizon.

From equation (3) we see that RMS velocities must be computed. We have utilized two approaches: I. The P-wave RMS velocities used in the migration may be obtained from the stacking velocity analysis of P-wave data. The S-wave RMS velocities may be estimated via the α/β relations and Dix' equation. More accurate S-velocities are achieved by migrating the data to S-S travel time depth, backing out the S-S velocity function in the migrated data and picking new migration velocities on S-S time scaled gathers.

II. Alternatively, RMS velocities are computed from P-wave interval velocities. Layers picked on the P-wave stack are assigned interval velocities and α/β ratios. S-wave interval velocities are computed via α/β and converted to RMS velocities. After migration, residual moveout in the image point gathers indicate inaccurate velocities. A layer stripping approach is convenient to update the P interval velocities. To achieve fast iterations, the migration scheme is restricted to a 1D velocity profile at a specific CDP location. When the all the events in the image point gather at the actual CDP location lines up horizontally, a reasonable choice of velocity parameters is achieved. The procedure should be repeated at several CDP locations to adjust for (mild) lateral changes in the parameter values.

Examples

Recently, a multicomponent acquisition technique for subsea seismic SUMIC was demonstrated by Berg et al. (1994a, 1996b). A 2D line was acquired over the diapiric Alpha structure at the Tommeliten field in the southern part of the North Sea. Hydrocarbon accumulations present in the Ekofisk and Tor formations of the Alpha structure, which correspond to Early Paleocene and Late Cretaceous ages, constitute the reservoir zone. A limited part of the overburden sediments

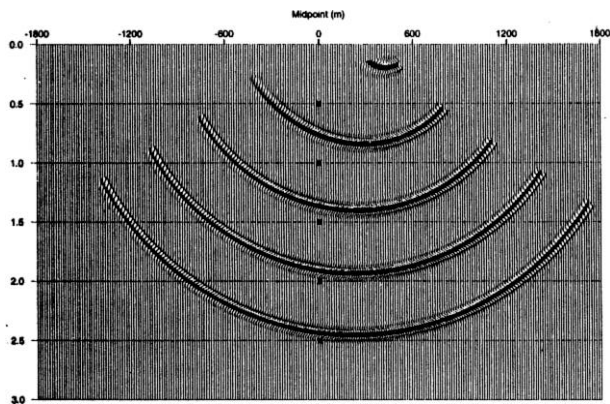


Figure 2: Migration impulse response with 60° dip limitation.

contain gas leaked out from the reservoir zone. The gas obviously slows down, attenuates and scatters the P-waves. Therefore, P-wave seismic do not map the reservoir zone, see Figure 3a. The mechanisms destroying the P-waves are not fully investigated. From Gassman's equations we know that the bulk modulus is much more affected by pore fluid type than the shear modulus. The objective of acquiring SUMIC data at Tommeliten was to see if S-waves could be used to give a confident image of the reservoir zone.

A detailed description of the SUMIC acquisition system can be found in Granli et al. (1995). SUMIC is a two boat operation. The shooting boat uses a conventional air gun source and passes over the recording sensors situated on the seafloor. Each sensor is equipped with three geophones oriented in the in-line, cross-line and vertical position to record the incident particle velocity wave field.

Granli et al. (1995) found that the main S-wave arrivals seen on the Tommeliten SUMIC in-line horizontal component are P-waves converted to S-waves in the subsurface. This conclusion was drawn from modelling results, well-log information, comparison with P-data sections and the static solutions obtained in the processing. Assuming an isotropic or vertical transversely isotropic medium, P to S converted waves will generate particle motion along the seismic line. Most of the shear-waves are recorded on the horizontal inline component, since low velocity layers near the sea bottom force the direction of S-wave propagation to be near vertical (even for large offsets) and by the fact that S-waves are polarized perpendicular to the propagation direction.

In Figure 3b the reservoir mapping obtained from P-SV DMO processing is shown. In Figure 3c the prestack time migration counterpart is presented. The P-SV images are superior to the vertical particle velocity image in Figure 3a in the uncertain zone. The P-waves are destroyed when entering the gas area, while the S-waves propagate relatively undisturbed through the gas. Coherent P-SV events are recorded as long as the down-going P-waves avoid the gas zone. Thus, intermediate-

to far-offset P-SV waves manage to undershoot the gas chimney and the "no-image-zone" is reduced.

Conclusions

A practical approach to prestack time migration of marine P-SV data has been demonstrated on Tommeliten field data. The zone of uncertain structural information is narrowed from approximately 2000 meter on the P-wave section to under 800 meter on the P-SV sections. Compared to PSDMO, the mapping of the uncertain zone using prestack migration are promising. Opposed to P-SV DMO, the scheme is based on very simple equations and explicit CCP sorting is avoided by going directly to the image domain.

In case of strong lateral velocity contrasts the migration scheme breaks down due to non-hyperbolic moveout in the image point gathers. Shales in the overburden are often severely transversely isotropic. Shear-wave data are strongly affected, since S-wave anisotropy is especially pronounced. Using a robust straight ray time migration scheme, the anisotropic behavior of the wave field is handled (although not very accurately) adjusting the RMS velocities to fit the moveout in the seismic data. A more subtle migration (e.g. depth migration) approach should take the anisotropy into consideration in order to succeed.

Acknowledgments

We want to thank John R. Granli and Eilert Hilde for their support in this work.

References

- [1] Berg, E., Svenning, B., Martin, J., 1994a, SUMIC: A New Strategic Tool for Exploration and Reservoir Mapping. Presented at the 56th annual EAEG meeting in Vienna.
- [2] Berg, E., Svenning, B., Martin, J., 1994b, SUMIC: Multicomponent Sea Bottom Surveying in the North Sea Data interpretation and Applications. Expanded Abstracts 64th Annual International Meeting Society of Exploration Geophysicists, 477-480.
- [3] Granli, J.R., Arntsen, B., Hilde, E. and Sollid, A., 1995, Imaging Through Gas Filled Sediments Using Marine S-wave Data. Paper presented at the 65th Annual Meeting Society of Exploration Geophysicists, Houston.
- [4] Harrison, M.P, 1992, Processing of P-SV Surface Seismic Data: Anisotropy Analysis, Dip Moveout, and Migration, Degree of Doctor of Philosophy, University of Calgary.
- [5] Tessmer, G., Behle, A., 1988, Common Reflection Point Data-stacking technique for converted waves. Geophysical Prospecting, 36, 661-668.
- [6] Fromm, G., Krey, T., and Wiest, B., 1985, Static and dynamic corrections, in Dohr, G. Ed., Seismic Shear Waves: Handbook of Geophysical Exploration, 15A, 191-225.

Prestack time migration of P-SV data

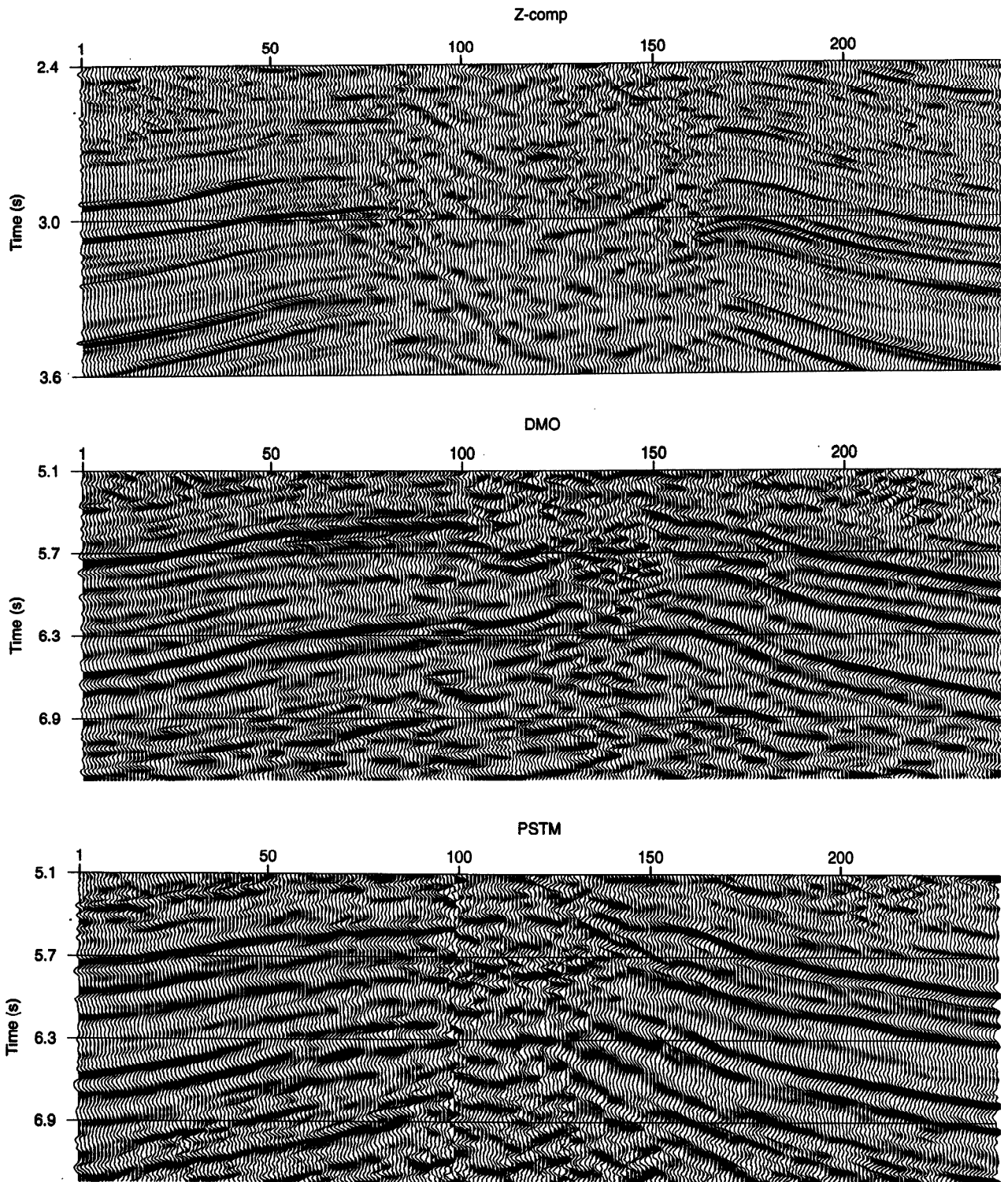


Figure 3: Stacked images of the Tommeliten Alpha structure. (a) Post-stack migrated vertical (Z) particle velocity data corresponding to P-wave data; (b) P-SV DMO and post-stack migration; (c) P-SV prestack time migration.